

Regulation of Xanthine Oxidase Activity by Substrates at Active Sites *via* Cooperative Interactions between Catalytic Subunits: Implication to Drug Pharmacokinetics

L.A. Tai and K.C. Hwang*

Department of Chemistry, National Tsing Hua University, Hsinchu, R. O. C., Taiwan

Abstract: Three xanthine oxidase substrates (i.e., xanthine, adenine, and 2-amino-4-hydroxypterin) show a “substrate inhibition” pattern (i.e., slower turnover rates at higher substrate concentrations), whereas another two substrates (i.e., xanthopterin and lumazine) show a “substrate activation” pattern (i.e., higher turnover rates at higher substrate concentrations). Binding of a 6-formylpterin at one of the two xanthine oxidase active sites slows down the turnover rate of xanthine at the adjacent active site from 17.0 s^{-1} to 10.5 s^{-1} , and converts the V -[S] plot from “substrate inhibition” pattern to a classical Michaelis-Menten hyperbolic saturation pattern. In contrast, binding of xanthine at an active site accelerates the turnover rate of 6-formylpterin at the neighboring active site. The experimental results demonstrate that a substrate can regulate the activity of xanthine oxidase via binding at the active sites; or a xanthine oxidase catalytic subunit can simultaneously serve as a regulatory unit. Theoretical simulation based on the velocity equation derived from the extended Michaelis-Menten model shows that the substrate inhibition and the substrate activation behavior in the V -[S] plots could be obtained by introducing cooperative interactions between two catalytic subunits in homodimeric enzymes. The current work confirms that there exist very strong cooperative interactions between the two catalytic subunits of xanthine oxidase.

Keywords: Cooperativity, 6-formylpterin, regulation, substrate inhibition, substrate activation, xanthine oxidase.

INTRODUCTION

In the study of enzyme kinetics, the Michaelis-Menten model, $E + S \rightleftharpoons [ES] \rightarrow E + P$, was commonly adopted to describe the kinetic behavior of single site enzymes. The velocity equation in the Michaelis-Menten model can be expressed by equation (1),

$$V = \frac{[E]_T \left(\frac{k_3[S]}{K_m} \right)}{\left(1 + \frac{[S]}{K_m} \right)} \quad (1),$$

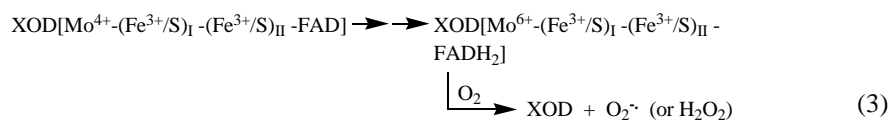
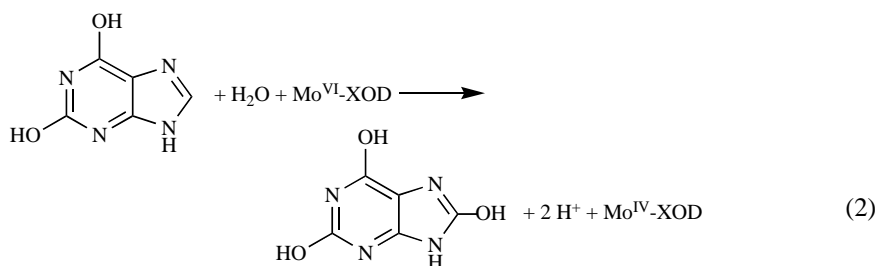
where [S] is the substrate concentration, V is the velocity, and K_m is the Michaelis constant. The Michaelis-Menten model predicts that the velocity, V , will increase hyperbolically to reach a maximum as the substrate concentration increases. The classical Michaelis-Menten model, however, cannot describe well the kinetics of enzymes with multiple catalytic subunits, of which the V -[S] plot very often shows non-hyperbolic saturation patterns; for example, sigmoidal shape [1], “substrate inhibition” behavior (i.e., gradual increase to reach a maximum, and then decrease at high substrate concentrations) [2,3], or “substrate activation” behavior (i.e., increase to reach a platform, and then further increase at high substrate concentrations) [4,5]. The substrate inhibition behavior in the V -[S] plot has been observed in many enzyme systems, such as, human prostatic acid phosphatase, and human glutathione synthetase [2,3]. The substrate activation behavior was observed in some other enzyme systems, such as, methylamine dehydrogenase and

acetylcholinesterase [4,5]. The substrate inhibition and substrate activation behaviors have never been observed in the same enzyme systems. The extreme case of substrate inhibition behavior was also known as the “half-of-the-sites” reactivity, that is, only half of the active sites in a homodimeric (or homo-tetrameric) enzyme can carry out catalysis at a time [6,7]. Many enzyme systems (such as, yeast glyceraldehyde-3-phosphate dehydrogenase and cytidine triphosphate synthetase), have been shown to exhibit “half-of-the-sites” reactivity behavior [6,7]. The origins of substrate inhibition and substrate activation phenomena are often attributed to the presence of a presumed peripheral regulatory site in the catalytic subunits [8,9]. At very high substrate concentration, substrate molecules start to bind to the reputed regulatory site, and feeds back to regulate (either activate or inhibit) the catalytic rate/ binding affinity of the substrate itself at the active site. Such type of substrate regulation of enzyme activity occurs only at very high substrate concentrations, and requires the presence of a regulatory site having low binding affinity toward substrates.

Xanthine oxidase (XOD) is a 290 kD homodimer protein having four cofactors in each monomer subunit, namely, a Mo(VI) ion at the active site, two 2Fe-2S clusters, and a FAD cofactor [10]. XOD activates a water molecule and inserts an oxygen atom into C-H bonds of many substrates, such as, xanthine and its analogs (see equations 2 & 3) [11].

The Mo(VI) ion at the active site is reduced to Mo(IV), which then transfers two electrons, via the 2Fe-2S clusters, to the FAD cofactor. The reduced flavin moiety then passes electrons to molecular oxygen to generate superoxide ($O_2^{\cdot -}$) or hydrogen peroxide (H_2O_2). Hydrogen peroxide can be further converted to the much more reactive hydroxyl radical ($\cdot OH$) by reducing metal ions (e.g., ferrous and cuprous ions). XOD is associated with many diseases (e.g., gout),

*Address correspondence to this author at the Department of Chemistry, National Tsing Hua University, Hsinchu, R. O. C., Taiwan; Tel/Fax: (+886) 3572 4810; E-mail: kchwang@mx.nthu.edu.tw



ischemia-reperfusion injuries, and inflammation in many diseases [12,13]. It was also demonstrated that XOD is capable of converting nitrates to nitric oxide (NO), a species well known to be involved in blood pressure regulation and immuno-response to antigens [14]. Understanding the mutual interactions between the two XOD catalytic subunits, and thus the catalysis/inhibition kinetics of XOD is very crucial to the development and pharmacokinetics of drugs (or inhibitors) for treatments of XOD-related diseases.

During the past 60 years, it was generally assumed that the two homo-catalytic subunits of XOD carry out catalysis independently [10,15,16]. However, many experimental results cannot be rationally explained by the independent catalysis model. For example, the turnover rate decreases at higher substrate concentrations (i.e., the “substrate inhibition” phenomenon) [17,18]. Previously, it was reported for the first time that there exist very strong cooperative interactions between the two homodimer subunits of XOD [19]. In this paper, we confirm the presence of strong cooperative interactions between the two XOD catalytic subunits. We show that both the substrate inhibition and substrate activation behaviors can occur in the xanthine oxidase system, which can be well described using the velocity equation derived from the extended Michaelis-Menten model [20]. The kinetic parameters indicate that there exist very strong cooperative interactions between the two XOD catalytic subunits, which lead to the observed substrate inhibition and substrate activation phenomena. Our data also demonstrate that enzyme activity can be regulated by substrates at active sites, and enzyme active sites can also simultaneously serve as regulatory sites.

RESULTS AND DISCUSSION

Cooperative interactions in the case of homo-substrates. Fig. (1a) shows the structures of five substrates used in this study. The star symbol indicates the position of the carbon atom where insertion of an oxo atom to the C-H bond occurs. The catalytic velocities of these substrates by XOD were measured individually (one substrate at a time) as a function of the substrate concentration in a PBS buffer solution at pH 7.5 and 22 °C. These catalysis velocities were normalized to the $2k_3[\text{E}_2]_0$ (i.e., V_{max}) value of individual substrate and plotted in the same figure for the purpose of comparison. As shown in Fig. (1b), three (i.e., xanthine, adenine, and 2-amino-4-hydroxypterin) of the five substrates show a so-called “substrate inhibition” behavior, i.e., the velocity

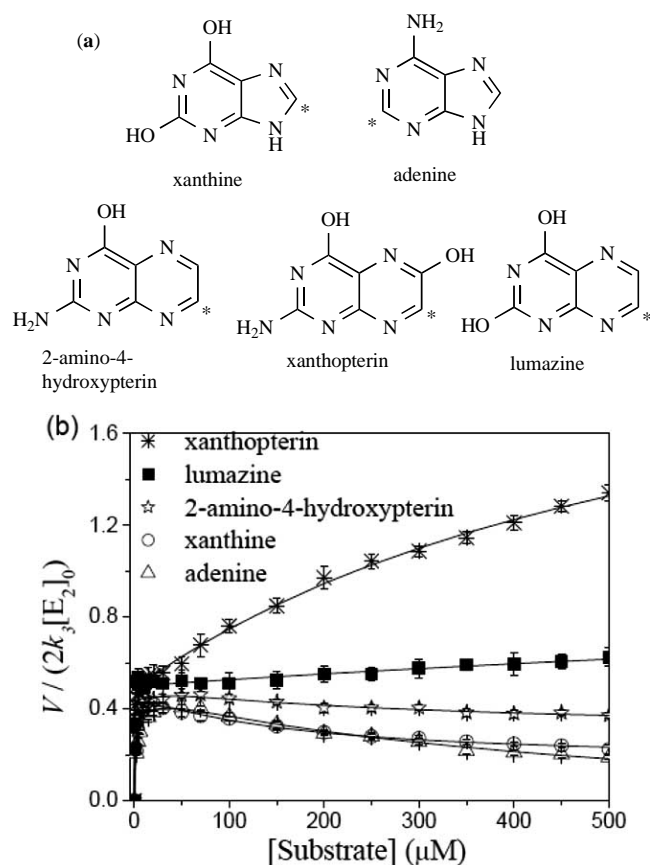
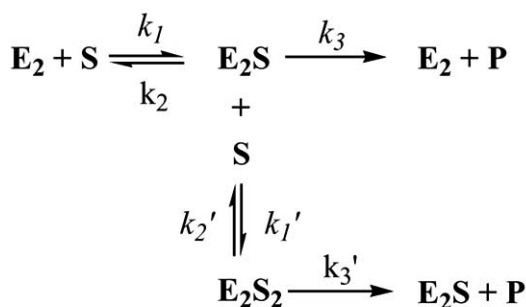


Fig. (1). (a) The structures of five substrates used in the studies. The star symbol labels the position of oxo atom insertion. (b) The normalized catalytic velocities of five different substrates as a function of the substrate concentrations. The catalytic velocities of all substrates were normalized to a local maximum of lumazine for the sake of easy comparison. The concentration of XOD functional active sites is in the range of 0.01 ~ 0.1 μM in a PBS buffer solution at pH 7.5 and 22 °C. The solid lines are calculated curves according to the equation (4) in the text. The values of the parameters K_m , k_3 , K_m' , and k_3' used to calculate the solid lines were listed in Table 1.

reaches a local maximum and then decreases at higher substrate concentrations. In contrast, the other two substrates (i.e., xanthopterin and lumazine) exhibit a “substrate activation” pattern, i.e., the velocity reaches a local maximum, and then further increases at higher substrate concentrations. Although both “substrate inhibition” and “substrate activation”



where $K_m = (k_2 + k_3)/k_1$; $K_m' = (k_2' + k_3')/k_1'$

Scheme 1. The balanced chemical equations for the extended Michaelis-Menten (or the Adair-Pauling) model, where the values of K_m , k_3 , K_m' , and k_3' have the usual meanings as those in the classic Michaelis-Menten model for single site enzymes. A simple kinetic derivation based on a *steady state condition* results in a velocity equation (4).

phenomena have been observed before in many enzyme systems, they were never observed to occur in the same enzyme. To rationalize the results shown in Fig. (1b), we applied the velocity equation (see equation (4)) derived from the extended Michaelis-Menten model [20] (see Scheme 1) to simulate the catalytic velocity, and compare with the experimental results shown in Fig. (1b). The k_m and k_3 values listed in Table 1 were used for the simulation curves (see the solid lines in Fig. (1b), which match with the experimental results the best. One of the unique features of the extended Michaelis-Menten model is that the values of K_m and k_3 for the first substrate molecule can be different from those (K_m' and k_3') of the second substrate molecule.

$$V = \frac{[E_2]_0 \left(\frac{k_3[S]}{K_m} + \frac{k_3'[S]^2}{K_m K_m'} \right)}{\left(1 + \frac{[S]}{K_m} + \frac{[S]^2}{K_m K_m'} \right)} \quad (4),$$

The values of K_m , k_3 , K_m' , and k_3' in the equation (4) can be systematically changed using the Origin software to look for a set of values having a minimum summation of difference between the calculated velocities and the experimental data at different substrate concentrations. The best-fit Michaelis constants and the turnover rates for the calculated curves are listed in Table 1 for the five substrates. In order to compare whether there are mutual interactions between the two XOD catalytic subunits, the kinetic parameters in Table 1 were converted to the intrinsic parameters of individual active site by the following relationships: $K_{m,intr} = 2 K_m$, $k_{3,intr} = k_3$, $K_{m,intr}' = 0.5 K_m'$, and $k_{3,intr}' = 0.5 k_3'$. From Table 1, we can see that pre-occupation of a homo-substrate at an active site often leads to a lower binding affinity (i.e., a larger value of $K_{m,intr}'$) at the adjacent XOD active site. In the cases of xanthine, adenine, and 2-amino-4-hydroxypterin, smaller turnover rates ($k_{3,intr}'$) were observed when a molecule of the same substrate binds at the adjacent active site. In the cases of xanthopterin and lumazine, the turnover rates ($k_{3,intr}'$), by contrast, increase from 0.24 to 0.69 s⁻¹, and from 1.0 to 1.1 s⁻¹, respectively, when a molecule of the same kind binds at the adjacent XOD active site. Different substrates have different catalytic rates (or the rate of oxo insertion to a C-H bond of a substrate), which is strongly related to the enzyme conformation and the substrate binding position at an active site. Conformational changes in an enzyme catalytic subunit induced by binding of a molecule at the adjacent catalytic subunit may lead to different binding affinity and catalytic rate at the active site being monitored. Decrease in the binding affinity (i.e., a larger $K_{m,intr}'$ value) may or may not be accompanied with decrease in the turnover rate, depending on the nature of the substrates and the way the conformation of a catalytic subunit being changed. In the case of xanthine, the far larger $K_{m,intr}'$ value (67.5 μM vs. original $K_{m,intr}$ of 4.6 μM) implies that pre-occupation of a xanthine molecule at an active site can effectively forbid entering of another xanthine molecule into the other active site. An extreme condition of this kind is the so-called “half-of-the-sites” reactivity [6,7], where only one of the two active sites can catalyze conversion of substrates at a time, and a homodimer

Table 1. Michaelis constants and turnover rates. The intrinsic values of Michaelis constant (K_m) and the turnover Rate (k_3) for an individual XOD active site was obtained under the condition of homo- and hetero-substrate cooperative interactions. All experiments were carried at 22°C and pH 7.5. For the definition of parameters, please see the Scheme 1.

Substrate	XOD ^[a]		XOD-S ₁ ^{[a],[b]}		XOD-6FP ^[c]	
	$K_{m,intr}$ (μM)	$k_{3,intr}$ (s ⁻¹)	$K_{m,intr}'$ (μM)	$k_{3,intr}'$ (s ⁻¹)	$K_{m,6FP}$ (μM)	$k_{3,6FP}$ (s ⁻¹)
Xanthine	4.6	17.0	67.5	2.75	5.0	10.5
Adenine	7.2	0.13	130	0.005	15.7	0.058
2-Amino-4-hydroxypterin	3.8	3.0	150	0.9	10.6	2.1
Xanthopterin	0.4	0.24	320	0.69	0.55	0.2
Lumazine	0.15	1.0	1000	1.1	0.73	0.62

[a] The kinetic parameters K_m , K_m' , k_3 and k_3' obtained from the extended Michaelis-Menten model were converted to the intrinsic parameters of each individual active site by the following relationships: $K_{m,intr} = 2 K_m$, $k_{3,intr} = k_3$, $K_{m,intr}' = 0.5 K_m'$, and $k_{3,intr}' = 0.5 k_3'$.

[b] XOD-S₁ represents that one of the two XOD active sites was pre-occupied by a substrate molecule of the same kind, which was being catalyzed by XOD.

[c] XOD-6FP₁ represents that one of the two XOD active sites was pre-occupied by a 6FP molecule. The terms $K_{m,6FP}$ and $k_{3,6FP}$ are the Michaelis-Menten constant and the turnover rate, respectively, for a substrate when one of the two XOD active sites was pre-occupied by a 6-formylpterin.

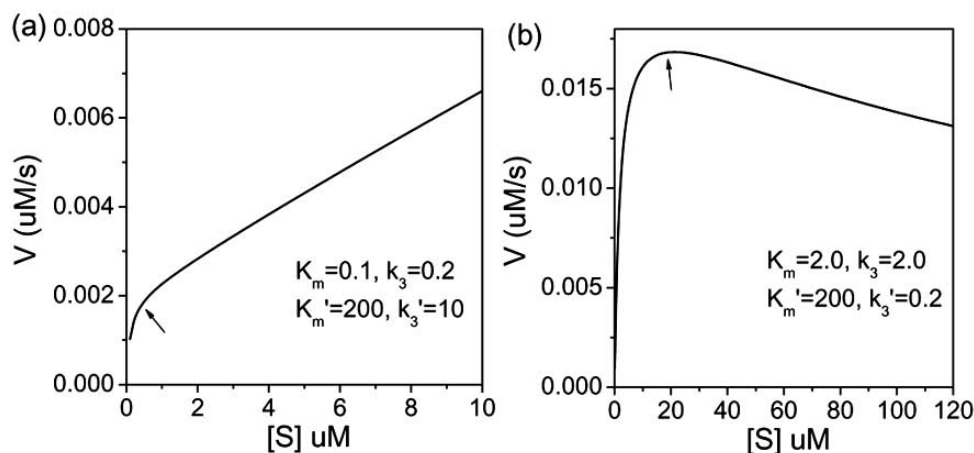
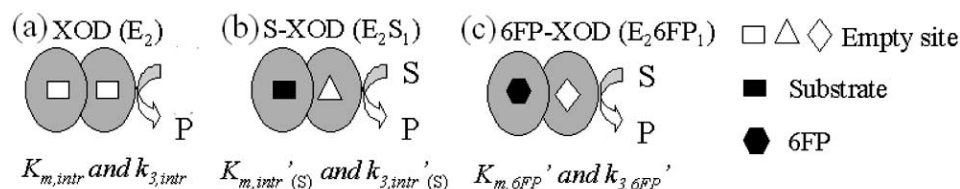


Fig. (2). Theoretical simulation using the velocity equation derived from the extended Michaelis-Menten model. **(a)** When k_3' is larger than k_3 , the V - $[S]$ plot shows a substrate activation pattern. **(b)** When the magnitude of k_3' is smaller than k_3 , the V - $[S]$ plot shows a substrate inhibition pattern. The magnitudes of k_m , k_m' , k_3 and k_3' used in the simulation are listed in the Figure. The location of arrow sign is a local maximum (or a transition point) in the velocity curve.

enzyme behaves in a manner similar to that of a single-site enzyme, that is, it follows the classic Michaelis-Menten kinetics for single-site enzymes and shows a hyperbolic saturation pattern in the V - $[S]$ plot. In the literature, observation of hyperbolic saturation curve in the V - $[S]$ plot was very often *mistakenly* used as a supporting evidence for the absence of cooperativity among enzyme subunits. Both the cases of “absence of cooperativity” and “super-strong negative cooperativity” (and the “half-of-the-sites” reactivity) follow the same (classic Michaelis-Menten) hyperbolic saturation pattern in the V - $[S]$ plot. In the case of XOD, only half of the active sites carry out their catalytic function under a low xanthine concentration ($< 67.5 \mu\text{M}$) condition. The current $k_{3,\text{intr}}$ value of 17.0 s^{-1} (at 22°C and $\text{pH } 7.5$, see Table 1) obtained using the above extended Michaelis-Menten model is nearly twice the literature value of 8.7 s^{-1} (at 25°C and $\text{pH } 7.5$) [21] which was obtained by assuming that two of XOD active sites carry out catalysis simultaneously, but, in fact, only one active site does catalysis. Therefore, the current $k_{3,\text{intr}}$ value of 17.0 s^{-1} represents the correct value of the turnover rate of an individual XOD subunit. Such an under-estimation in the value of k_3 most probably also occurs in many other oligomeric enzyme systems. Our results demonstrate a few salient features: (a) substrates can regulate an enzyme’s activity via binding at active sites; (b) a catalytic subunit of an oligomeric enzyme can simultaneously serve as a regulatory subunit; and (c) the mode of regulation is determined by the structure of the substrates, instead of the location of the regulatory site.

The velocity equation derived from the extended Michaelis-Menten model [20] (see Scheme 1 and the equation (4)) includes both positive and negative cooperative interactions, as well as non-cooperative interaction between two catalytic subunits. In the case of non-cooperative interaction, the values of K_m and k_3 (for the first active site) are equal to those of K_m' and k_3' (for the second active site), respectively. Based on the velocity equation (4), we did theoretical simulation to identify the effects of relative magnitudes of K_m , K_m' , k_3 and k_3' on the catalytic pattern. From the simulation, we found that the catalysis patterns in the V - $[S]$ plot are solely determined by the relative magnitude of k_3' to k_3 .

When k_3' is larger than k_3 (i.e., binding of the first substrate molecule at an active site A accelerates the catalysis rate at the adjacent active site B), the V - $[S]$ plot shows a substrate activation pattern. In other words, the catalysis velocity reaches a local maximum, and then further increases at higher substrate concentrations (see, Fig. (2a)). When k_3' is smaller than k_3 (i.e., binding of the first substrate molecule at an active site A slows down the catalysis rate at the adjacent active site B), the V - $[S]$ plot shows a substrate inhibition pattern. That is, the catalysis velocity reaches a local maximum, and then further increases at high substrate concentrations (see, Fig. (2b)). The magnitudes K_m and K_m' do not affect the catalysis pattern, but determines the location of the local maximum point (or a transition point) in the V - $[S]$ plot (see the arrow signs shown in Fig. (2a) & (2b)). When K_m' is far smaller than K_m (i.e., $K_m' \ll K_m$), binding of the first substrate at an active site dramatically promotes binding of a second substrate at the other active site, and the local maximum (or the transition point) appears at low substrate concentration regime. In such a case, the enzyme substrate complex E_2S_2 is predominantly formed over the E_2S form. At very high substrate concentrations, the contribution of the $[S]/K_m$ term in the equation (4) becomes negligible as compared to the $[S]^2/K_mK_m'$ term. The velocity, V , now approaches the value of $k_3'[E_2]_0$, which is the final limiting value of the velocity at extremely high substrate concentrations. Overall, as the substrate concentration is increased from low to very high, the dominant catalysis species switches from E_2S to E_2S_2 . The velocity (V) increases gradually, through a hyperbolic saturation region, to reach a local maximum where the dominant catalysis species is the E_2S , and then further approaches the ultimate limit value, $k_3'[E_2]_0$. If the E_2S_2 species has a slower catalytic rate than does E_2S (i.e., $k_3' < k_3$), the velocity will decrease from the local maximum to approach the smaller final $k_3'[E_2]_0$ value. This case accounts for the commonly observed “substrate inhibition” behavior. From the results in Fig. (1) and Table 1, one can see that the $k_{3,\text{intr}}$ values of xanthine, adenine and 2-amino-4-hydroxypterin (see the middle, homo-substrate column in Table 1) all are smaller than their individual k_3 values obtained at very low substrate concentrations. There-



Scheme 2. Schematic representation of homodimer enzymes having catalysis rate and turnover rate for substrate S when the adjacent active is (a) empty, (b) occupied by the same substrate, S; or (c) occupied by a hetero-substrate, P.

fore, these three substrates show a “substrate inhibition” behavior. If the E_2S_2 species has a faster catalytic rate than does E_2S (i.e., $k_3' > k_3$), the velocity will further increase from the local maximum (or the transition point indicated by an arrow, see Fig. (2a)) and approach to the larger final $k_3'[E_2]_0$ value. This case accounts for the commonly observed “substrate activation” phenomenon. As shown in Fig. (1) and Table 1, the $k_{3,intr}'$ values of xanthopterin and lumazine (see the middle, homo-substrate column in Table 1) all are larger than their individual k_3 values obtained at very low substrate concentrations. Therefore, these two substrates lead to a “substrate activation” behavior. Our simulation results indicate that the key factor determining substrate inhibition or substrate activation is the relative magnitude of $k_3'[E_2]_0$ to $k_3[E_2]_0$, but not by the relative magnitude of K_m to K_m' . A larger K_m' value than K_m simply shifts the local maximum location (or the local V_{max} in the V -[S] plot) toward a higher substrate concentration region. For a system of $K_m' < K_m$, the local V_{max} will shift to a smaller substrate concentration region in the V -[S] plot. The simulation results are consistent with the experimental observation shown in Fig. (1) and Table 1.

In the literature, the “substrate inhibition” and “substrate activation” phenomena were often rationalized by assuming that a substrate molecule might also serve as a regulator by binding at a reputed peripheral regulatory site [8,9] at very high substrate concentrations. The presence of a peripheral regulatory site was observed in the AChE [22,23], Bromelain/Papain [24,25] systems, but was never observed in XOD. By using the extended Michaelis-Menten model, the substrate inhibition and substrate activation phenomena can be well described and understood as a natural consequence of cooperative interactions between two active sites. It is not necessary to assume the presence of a reputed peripheral regulatory site. The presumed regulatory site in each catalytic subunit, however, has never been proven to exist experimentally in the XOD system. An XOD crystal was successfully grown in complex with an inhibitor, salicylate [10,26]. In the 3D crystal structure, the inhibitor molecule was found at the two XOD active sites only, and no other peripheral binding site was found. In another studies, a crystalline structure of XOD in complex with a slow substrate, namely, 2-hydroxy-6-methylpurine, was obtained [27]. The crystalline structure shows that the two XOD catalytic subunits have slightly different conformations and the substrate molecules in the two active sites are in different catalytic stages, indicating that the two XOD catalytic subunits take turn in catalysis motion, with the first one in action and the other resting [27]. The result implies that there exists some cooperative relationship between the XOD active sites (or subunits). In an inhibition experiment, it was found that the amount of alloxanthine bound to XOD enzyme was pro-

portional to the percentage of functional XOD active sites in a nearly 1:1 stoichiometric ratio [28]. All these results indicate the absence of any peripheral binding site in each XOD subunit. In addition, the cooperative interaction between the two XOD active sites was previously proved experimentally [19]. At very high substrate concentrations (beyond the K_m value), two substrate molecules can bind to the two adjacent XOD active sites simultaneously. Occupancy of a substrate at an active site might result in changes in the protein conformation of the adjacent subunit, leading to dynamic changes in the substrate binding affinity, as well as turnover rate, at the adjacent catalytic site during the short time period of substrate residence at the other active site (see cartoon pictures in Scheme 2). As schematically represented in the Scheme 2, the catalytic properties of an active site might be changed (or regulated) according to the binding states (a), (b), and (c) of an adjacent active site. An extreme condition of “substrate inhibition” behavior could lead to “half-of-the-sites” reactivity [6,7].

Cooperative interactions in hetero-substrates. The extended Michaelis-Menten model shown in Scheme 1 can be extended to hetero-substrates (i.e., two different substrates, S_1 and S_2 , instead of 2 moles of the same substrates, S); the cooperative catalysis model for the interactions of hetero-substrates can also be derived in a similar, but more-complicated, manner [29]. In addition to the cooperative interaction observed for homo-substrates, hetero-substrates cooperative interaction can also be observed in the XOD system at low substrate concentrations. When one of the two XOD active sites is pre-occupied by a substrate, the binding and catalytic functions of the adjacent active site change dramatically [19]. One can use an inhibitor-like substrate (such as, 6FP) to occupy one of the two XOD active sites and prepare a “quasi-single site” enzyme for catalysis of other substrates at the other active site. During the very short period of turnover time, the slow-conversion of the inhibitor-like substrate will not be converted to products and leave the active site. Therefore, the “quasi-single site” enzyme will follow the classic Michaelis-Menten hyperbolic saturation catalytic pattern. As displayed in Fig. (3a), the conversion rate of xanthine to uric acid was significantly retarded by pre-occupation of 6FP at the adjacent XOD active site, and the V -[S] plot was changed from substrate inhibition to a hyperbolic saturation pattern. A similar phenomenon was also observed for adenine (see Fig. (3b)) as well as the other three XOD substrates (see results in Table 1). 6FP can bind to the XOD active sites nearly quantitatively and irreversibly, that is, 6FP can bind to each active site with a large association constant ($k_1 = 1.1 \times 10^6 \text{ M}^{-1}\text{s}^{-1}$), but a very small dissociation constant ($k_2 = 0.7 \times 10^{-4} \text{ s}^{-1}$) for the enzyme-substrate complex [19]. In the presence of 0.75 equivalent (relative to the XOD functional active sites) of 6FP, the rela-

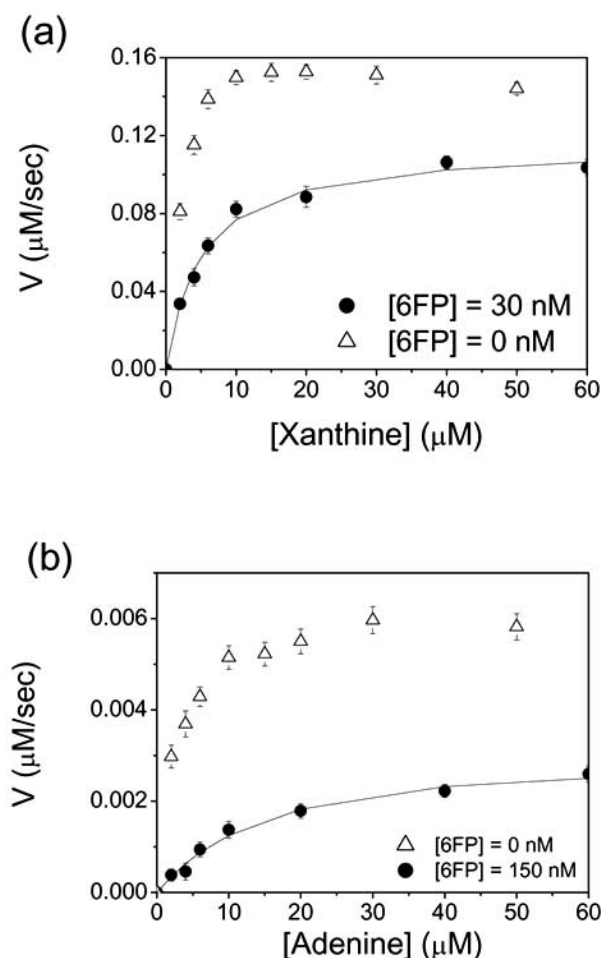


Fig. (3). (a) The catalytic velocity of xanthine as a function of the xanthine concentration in the absence (Δ) and the presence (\bullet) of 6-formylpterin (30 nM). The concentration of XOD functional active sites is 40 nM in a PBS buffer at pH 7.5 and 22 °C. Xanthine of different concentrations was added to the solution 1 min after mixing 6FP with XOD (see the text for discussion). The solid line was calculated according to the equation (3) in the text using a set of parameters (K_m , k_3) of (5.0 μM , 10.5 s^{-1}). (b) The catalytic velocity of adenine as a function of the adenine concentration in the absence (Δ) and the presence (\bullet) of 6-formylpterin (30 nM).

tive quantities of all enzyme intermediates at the mid-time (i.e., at 30 seconds after mixing) of the measurement are 7.3 %, 40.6%, and 52.1 %, for free XOD, XOD-6FP₁, and XOD-6FP₂, respectively. These relative percentages were calculated based on the kinetic constants of 6FP with XOD (see the experimental section for the calculation). The XOD concentration used to fit the experiment data is the sum of XOD and XOD-6FP₁. Therefore, a majority of the XODs are in the form of XOD-6FP₁ during the time period of rate measurements in Fig. (3). One can ignore the XOD-6FP₂ species since it does not have any empty active site available for substrate catalysis and thus will not contribute to the enzymatic conversion of xanthine to uric acid. The contribution from the small amount of free XOD (with two free active sites) was neglected for the moment for the sake of simplicity. The half-life of XOD-6FP₁ is ~13 minutes [19], a time scale far longer than a turnover cycle of most XOD substrates. The XOD-6FP₁ form can, therefore, be treated as a

quasi-single-site enzyme, and the experimental turnover rates of xanthine to uric acid can be analyzed using the classic Michaelis-Menten equation (i.e., the velocity equation (1)). Reprocessing the data in Fig. (3) in the form of a Lineweaver-Burk plot ($1/V$ vs. $1/[S]$), one obtains a Michaelis constant ($K_{m,6FP}$) and a turnover rate ($k_{3,6FP}$) of 5.0 μM and 10.5 s^{-1} , respectively, for xanthine. The solid line was calculated according to equation (1) using a set of parameters (K_m , k_3) of (5.0 μM , 10.5 s^{-1}). These values have an uncertainty of ~15%, due mainly to the variation in the concentration of XOD-6FP₁ during the time period of the experiments and the influence of a small amount of free XOD. When compared to the values of 4.6 μM and 17.0 s^{-1} (see Table 1) obtained under a very low xanthine concentration and the absence of 6FP, it is very clear that pre-occupation of 6FP at one XOD active site results in a nearly the same binding affinity, but a slower turnover rate of xanthine at the adjacent active site. Similar experiments were carried for the other four XOD substrates, and the measured rate constants were listed in Table 1 (see the 6FP effects column in Table 1). It can be seen that pre-occupation of a 6FP leads to retardation in both the binding affinities and the turnover rates for all five substrates, but to different extent.

Although the substrate inhibition/ activation phenomena observed in the XOD system can be well explained by the cooperative interactions between two catalytic subunits as predicted by the extended Michaelis-Menten model, we can further evaluate the possibility whether these phenomena can be due to the formation of ternary complexes between two substrate molecules and a XOD subunit, i.e., there exists a peripheral regulatory site at each XOD catalytic subunit. Experimentally, it is quite difficult to differentiate the ternary complex model from the cooperative interaction model (i.e., two substrates bound at two different subunits which have strong cooperative interactions). We can first assume that there exists a peripheral regulatory site at each XOD catalytic subunit, and then disprove the assumption. The “substrate activation” and “substrate inhibition” phenomena occur at high substrate concentrations, indicating that substrate binding to the peripheral regulatory site takes place only at high substrate concentrations. If a substrate preferentially bind to the peripheral site prior to the active site, a classic Michaelis-Menten hyperbolic saturation curve in the V - $[S]$ plot should be observed, instead of the substrate activation/ inhibition types of catalysis patterns. In other words, the portion of substrate-binding to a peripheral site, if any, is negligible at very low substrate concentrations. With such an understanding in mind, we go back to examine the experimental data in Fig. (3). The experimental data show that the presence of 0.75 eq. of 6FP, a very low concentration of 30 nM, leads to change of the catalytic pattern of xanthine from the “substrate inhibition” pattern to classic Michaelis-Menten hyperbolic saturation. Two situations could possibly lead to such a change in the catalysis pattern. The first possible situation is that all peripheral sites in XOD homodimers were occupied by 6FP and no cooperative interactions between the two XOD catalytic subunits. This situation does not exist since the amount of 6FP used is less than one equivalent (relative to XOD active sites). If there exists a peripheral site in each XOD subunit, there is no way one can use less than one eq. of tight binding substrate (such as, 6FP) to com-

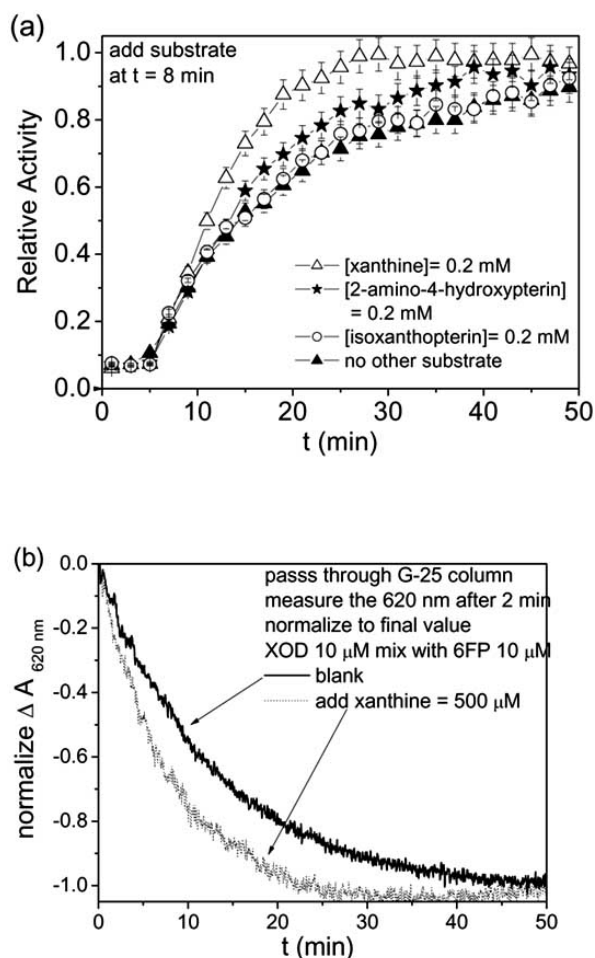


Fig. (4). Normalized XOD activity as a function of time in the presence of different substrates: (a) 0.2 mM xanthine (Δ); 0.2 mM 2-amino-4-hydroxypterin (\star); 0.2 mM isoxanthopterin (\circ); and the absence of other substrate (\blacktriangle). The XOD solution (pH 7.5 in a 0.1 M PBS buffer at 22 $^{\circ}\text{C}$) was pre-mixed with 1 equivalent of 6FP to form XOD-6FP₂ complex. 0.2 mM of hetero substrate was added 8 min after adding the solution to affect the conversion of 6FP to 6CP. 20 μL of the enzyme solution was removed and added to a 2 mL solution containing 50 mM xanthine to examine for its activity. (b) The bleaching rate at 388 nm in the absence (solid line) and the presence (dot line) of 0.5 mM xanthine. An aliquot of xanthine solution was added to the XOD solution after mixing of XOD and 6FP.

pletely occupy all peripheral (regulatory) site and convert the substrate activation/ substrate inhibition catalysis pattern to classic Michaelis-Menten hyperbolic pattern. In addition, we previously observed that addition of 1–4 eq. 6FP to a XOD solution leads to a formation of ES complexes having a charge transfer band absorption at 620 nm [24], and these bound 6FP could be converted to 6-carboxypterine (6CP) quantitatively, indicating that the binding location of 6FP is the active site [19]. The experimental data in Fig. (3) has completely excluded the possibility of existence of a peripheral site in each XOD catalytic subunit. The second possible situation is the absence of a peripheral site in each XOD subunit, but accompanied with strong cooperative interactions between the two XOD catalytic subunits. Under such a condition, less than one eq. of an inhibitor-like substrate can

occupy part of active sites, generating some quasi-single site XOD homodimer enzyme species with one empty site and the other occupied. If there is absence of any sort of cooperative interactions between the XOD subunits (i.e., independent catalysis for each subunit), one would obtain a classic Michaelis-Menten hyperbolic saturation pattern with the same catalytic parameters (Michaelis constant and turnover rates). This case does not match with the experimental results shown in Fig. (3). Overall, the only situation, which can explain our experimental observation, is the absence of a peripheral site in each XOD subunit and simultaneous existence of strong cooperative interactions between the two XOD subunits. The conclusion is supported by the x-ray crystallography results and our previous observation of cooperativity in the XOD system [19]. Besides xanthine, four other XOD substrates (i.e., adenine, 2-amino-4-hydroxypterin, xanthopterin, and lumazine) all change from their original substrate inhibition/ activation pattern to a classic Michaelis-Menten hyperbolic saturation pattern in the presence of 0.75 eq. of 6FP (results in Table 1). Therefore, the data in Fig. (3) does not support the assumptions of existence of a peripheral regulatory site in each XOD subunit and the absence of cooperative interactions between XOD subunits, but can be well explained by the cooperative interaction model. The data in Figs. (1 and 3) demonstrate that strong cooperative interactions between the two XOD subunits can result in “substrate activation” and “substrate inhibition” catalysis patterns. More importantly, the XOD system demonstrates a unique enzyme regulation mechanism via binding of its substrates at active sites.

Regulation of enzyme activities by substrates at active sites. As shown above, pre-occupation of a 6FP molecule at an XOD active site can change the catalytic behavior of the neighboring catalytic subunit. Simultaneously, the substrate at the second active site of the neighboring catalytic subunit can also alternate the rate of catalysis of the pre-occupied 6FP at the first active site. In fact, two of the same or different substrates at the two XOD active sites have mutual regulation effects on each other. In other words, an XOD catalytic subunit can simultaneously serve as a regulatory unit as well for the adjacent subunit(s). In Fig. (3), we observe that the binding of 6FP could slow down the turnover rate of xanthine at the adjacent active site from 17.0 to 10.5 s^{-1} (see Table 1). By contrast, the presence of xanthine at the XOD active site was observed to accelerate the conversion of the pre-occupied 6FP to 6-carboxypterin (6CP) as evidenced by the enhanced activity recovery rate and faster disappearance of the 6FP-XOD charge transfer band at 620 nm (see Figs. 4(a) & 4(b)). Other substrates, such as 2-amino-4-hydroxypterin, and isoxanthopterin, were also observed and able to accelerate the conversion of 6FP to 6CP, but to different extent. To accelerate the conversion of 6FP to 6CP, the hetero substrates could bind to the only available free active site of the XOD-6FP₁ species and affect the catalytic rate of XOD-6FP₁ via cooperative interaction between the two XOD subunits. The acceleration effect of xanthine is larger than that of 2-amino-4-hydroxypterin at the same concentration of 0.2 mM, which is consistent with the smaller $K_{m,6FP}$ of xanthine (5.0 μM) than 2-amino-4-hydroxypterin (10.6 μM , see Table 1). A smaller $K_{m,6FP}$ of xanthine means that a larger portion of the only available active site of XOD-

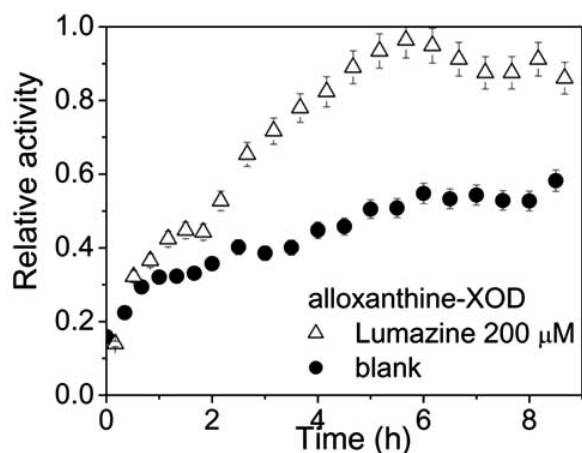


Fig. (5). The recovery of the XOD activity from an alloxanthine-XOD(Mo^{4+}) complex solution in 0.1 M phosphate at pH 7.5 in the presence (Δ) and the absence (\bullet) of 200 μM lumazine at 22 $^{\circ}\text{C}$ in air. The alloxanthine-XOD(Mo^{4+}) complex solution was obtained by mixing a XOD solution with excess amount of allopurinol, followed by passing the solution through a Sephadex G-25 column to isolate the alloxanthine-XOD(Mo^{4+}) complex. The XOD activity was monitored by removing an aliquot of the XOD solution every 20 min to examine for its activity using xanthine as a substrate.

6FP₁ species will be occupied by xanthine than by 2-amino-4-hydroxypterin at the same concentration, and thus larger portion of XOD-6FP₁ was accelerated to the product in the presence of xanthine. The accelerated product formation of XOD-6FP₁ is also evidenced by the faster 6CP formation (i.e., bleaching at 620 nm) in the presence of xanthine (see Fig. (4b)). The argument of cooperativity between two XOD active sites was also supported by lumazine-accelerated activity recovery rate of alloxanthine-inhibited XOD (see Fig. 5). Allopurinol is a XOD substrate, and can be converted to a potent XOD inhibitor, namely, alloxanthine, which then binds the reduced form of XOD($-\text{Mo}^{4+}$) [28]. Mixing of XOD with allopurinol will lead to complete inhibition of XOD by alloxanthine. The alloxanthine-inhibited XOD has a half-life of ~ 5 hr. As shown in Fig. (5), the presence of 0.2 mM lumazine significantly accelerates the activity recovery rate of the alloxanthine-inhibited XOD and shortens its half-life from 5 hr to ~ 2 hr. The results in Figs. (4 & 5) unambiguously show that there indeed exists a very strong cooperative interactions between the two XOD subunits, and the presence of a second substrate can tune (or regulate) the catalytic pattern of XOD for other substrates. In general, the substrate-regulation phenomenon would be enhanced and readily observed if one or both of the two substrates are slow (or inhibitor-like) XOD substrates, and thus have a longer residence time (or smaller turnover rate) at active sites. Allopurinol is the current clinical medicine for treatment of gout. Based on the previous assumption of independent catalysis of XOD active sites, the subsequent metabolized product of allopurinol (i.e., alloxanthine) will bind to and inhibit the two XOD active sites independently. As shown in the Fig. (5), the dissociation half life of the alloxanthine-XOD complex changes dramatically from ~ 5 h to ~ 2 hr in the presence of XOD substrates. In the in-vivo systems, XOD substrates are abundant in biological tissues/organs, which will change the pharmacokinetics and thus the efficacies of allopurinol dramatically. Currently, the true mecha-

nisms how allopurinol inhibits XOD and how the alloxanthine-XOD complex is re-activated are still largely unknown. To have proper doses of allopurinol for treatments of gout and other XOD related diseases, it is necessary to figure out how XOD was inhibited and re-activated by its inhibitors (or medicinal molecules) by taking into account of the cooperative interactions between the two XOD catalytic subunits.

CONCLUSION

In summary, we have observed the substrate inhibition and substrate activation phenomena occur simultaneously in xanthine oxidase. The substrate inhibition pattern can be converted to the classical Michaelis-Menten hyperbolic saturation pattern by the presence (or binding) of an inhibitor-like substrate, i.e., 6-formylpterin, in one of the two XOD active sites. The substrate inhibition and substrate activation phenomena can be well simulated using the velocity equation derived from the extended Michaelis-Menten model by introducing cooperative interactions between two catalytic subunits in homodimeric enzymes. In other words, strong cooperative interactions between catalytic subunits of an enzyme could be the origin of commonly observed phenomena of substrate inhibition and substrate activation, without the necessity to assume the presence of a peripheral regulatory sites (or unit). The previous discovery that there are very strong cooperative interactions between the two XOD catalytic subunits was further confirmed. This work also demonstrated that the half life of the XOD-inhibitor (i.e., alloxanthine) complex was significantly shortened from ~ 5 h to ~ 2 h in the presence of XOD substrates. Since XOD is involved in many important diseases, such as, gout, ischemia reperfusion injury, nitric oxide formation, understanding the details of cooperative interactions between the two XOD catalytic subunits is crucial to the pharmacokinetics and treatments of the XOD related diseases, and will shed light on the future drug design.

MATERIALS AND METHODS

General procedure for turnover rate measurements. The enzyme purification procedure was described in detail in [19]. Briefly, the commercial XOD (*Calbiochem*, ~ 40 % activity) was purified via an EAH-SepharoseTM 4B/folate column (39) to a ~ 85 % purity level. The concentration of functional active sites of XOD was determined by the AFR^{25°C} method [30]. In a typical experiment, the concentration of XOD functional active sites was in the range of 0.01 \sim 0.1 μM in a PBS buffer solution at pH 7.5 and 22 $^{\circ}\text{C}$. The velocity of each substrate was obtained from the slope in the plot of product absorbance vs. time. The absorbance was measured at a particular wavelength where the absorbance of a product was large and there was a minimal interference from the reactant substrate. The monitoring wavelengths for different substrate-product systems are listed below: 294 nm ($\Delta\epsilon_{\text{product-substrate}} = \Delta\epsilon_{294\text{nm}} = 11200 \text{ M}^{-1}\text{cm}^{-1}$) for xanthine, 305 nm ($\Delta\epsilon_{305\text{nm}} = 11800 \text{ M}^{-1}\text{cm}^{-1}$) for adenine, 294 nm ($\Delta\epsilon_{294\text{nm}} = 4530 \text{ M}^{-1}\text{cm}^{-1}$) for 2-amino-4-hydroxypterin, 310 nm ($\Delta\epsilon_{310\text{nm}} = 7180 \text{ M}^{-1}\text{cm}^{-1}$) for xanthopterin, and 284 nm ($\Delta\epsilon_{284\text{nm}} = 5030 \text{ M}^{-1}\text{cm}^{-1}$) for lumazine. In general, the absorption coefficient of a substrate at the monitoring wavelength was between 20 $\text{M}^{-1}\text{cm}^{-1}$ and 2020 $\text{M}^{-1}\text{cm}^{-1}$. An aliquot of a XOD aqueous solution was added into a substrate

containing solution to initiate the enzyme reaction. The velocity at a given substrate concentration was obtained from the slope at the first 30 to 200 second in the absorbance-time plot, where consumption of substrate is usually below 10 %. The above experiments were carried out at different substrate concentrations. The observed initial velocity was then plotted as a function of the substrate concentration. Unless otherwise mentioned, all initial velocity measurements were repeated three times and the average values were reported.

The turnover rate from the “quasi-single-site” XOD-6FP₁ enzyme species. Xanthine oxidase is a homodimer enzyme. In order to prepare a quasi-single site XOD enzyme species and study the catalytic activity of such a quasi-single site enzyme, 0.75 equivalent of 6FP was added to a XOD aqueous solution. By comparing the catalysis rates of free XOD and quasi-single site XOD species toward the same substrate, one can obtain information regarding how a bound substrate (here, 6FP in this case) at one of the two XOD active sites affect the catalysis rate of the other active site. In the presence of 0.75 equivalent (relative to XOD functional active sites, unless otherwise mentioned) of 6FP, XOD will exist in the forms of XOD, XOD-6FP₁, and XOD-6FP₂ [19]. Binding of 6FP to XOD active sites is nearly quantitative and is irreversible with dissociation half life of ~17 minutes, due to the very small dissociation rate constants (k_2 and k_2' in Scheme 2 in the results and discussion section), on the order of 10^{-4} ~ 10^{-5} s⁻¹. The enzymatic conversion rates (k_3 , and k_3') of 6FP to 6-carboxylpterin (6CP) from XOD-6FP₁, and XOD-6FP₂ are 0.95×10^{-3} and 2.8×10^{-3} s⁻¹, respectively [19]. After addition of XOD to an aqueous solution containing 0.75 equivalent 6FP, the solution was incubated for 10 seconds to allow formation of XOD/6FP complexes. In the presence of 0.75 equivalent of 6FP, XOD and 6FP will form complexes and reach equilibrium within a few seconds after mixing. XOD molecules will populate among the forms of free XOD, XOD-6FP₁, and XOD-6FP₂ with a ratio of 6.25%, 37.5%, and 56.25%, calculated based on a statistic distribution (for the sake of simplicity, the effect of cooperative interactions on the distribution of XOD/6FP complexes is neglected here). Distribution of the above three enzyme species will slowly change as time proceeds. The XOD-6FP₂ will gradually convert to XOD-6FP₁ by following the equation, $[XOD-6FP_2] = [XOD-6FP_2]_0 \exp(-k_3' t)$. Whereas, XOD-6FP₁ will gradually convert to free XOD by following the equation, $[XOD-6FP_1] = [XOD-6FP_1]_0 \exp(-k_3 t)$. Therefore, the amount of free XOD, XOD-6FP₁, and XOD-6FP₂ at a particular time after mixing of 6FP and XOD can be calculated by the following equation (5)

$$[XOD-6FP_2] = [XOD-6FP_2]_0 \exp(-k_3' t) \quad (5a)$$

$$[XOD-6FP_1] = [XOD-6FP_1]_0 \exp(-k_3 t) + [XOD-6FP_2]_0$$

$$[1 - \exp(-k_3' t)] \exp(-k_3 t) \quad (5b)$$

$$[XOD] = [XOD]_0 + \{[XOD-6FP_1]_0 + [XOD-6FP_2]_0$$

$$[1 - \exp(-k_3' t)]\} [1 - \exp(-k_3 t)] \quad (5c)$$

Overall, at 60 seconds after mixing 0.75 equivalent of 6FP with XOD, the distribution of free XOD, XOD-6FP₁, and XOD-6FP₂ becomes 8.83 %, 43.62 %, and 47.55%, respectively. The XOD-6FP₂ does not have any available ac-

tive sites for substrate binding and catalysis. The dominant catalytic species in the solution is the XOD-6FP₁, which has only a single active site available for other substrates and can be used to investigate the catalysis behavior of very fast substrates. For fast substrates (such as, xanthine and xanthopterin) the turnover time is very short, on the order of a few tenths of mini seconds. The product formation velocities were monitored for 30 seconds after the mixing of substrates and enzyme. All kinetic observation was done within one minute. Within one minute, the conversion of xanthine to uric acid by XOD ends, but the distribution of free XOD, XOD-6FP₁, and XOD-6FP₂ does not change significantly. During this short time period, only less than 10 % of 6FP was converted to 6CP. Since XOD-6FP₂ has no empty active site and could not catalyze conversion of xanthine to uric acid, uric acid was formed mainly from the XOD-6FP₁ (in the amount of ~85%) and the free XOD (in an amount of ~15%). The classic Michaelis-Menten equation was adopted to obtain the $K_{m,6FP}$ and $k_{3,6FP}$ value for this “pseudo-single site” XOD-6FP₁ enzyme species. The turnover rate of xanthine by the XOD-6FP₁ species was obtained by subtracting the ~15% contribution from the free XOD species of which the turnover rate is known and can be measured separately. The experiments were done at different xanthine concentrations in order to collect enough data points for the V - [S] plot.

The conversion of 6FP to 6CP by XOD in the presence of other substrates. In the previous section, the effect of a bound 6FP on the catalytic behavior of the other XOD active site was studied. In this section, experiments were designed to study the reverse effect, namely, the effects of substrate binding (at an XOD active site) on the catalysis behavior of 6FP bound at the adjacent XOD active site. The XOD solution (pH 7.5 in a 0.1 M PBS buffer at 22 °C) was pre-mixed with 1.2 equivalent of 6FP to form the XOD-6FP₂ complex. Another substrate with final concentration of 0.2 mM was added to the solution at 8 minutes after addition of 6FP to affect the conversion of 6FP to 6CP. In order to determine the effect of other substrates on the turnover rate of the 6FP to 6CP by the XOD-6FP₁ species, 20 μ L of the 6FP/XOD solution was removed and added into a 2 mL solution containing 50 μ M xanthine to measure the enzyme activity. Notice that the turnover rate of 6FP to 6CP from the XOD-6FP₂ species is not expected to be influenced by the presence of other substrates, since XOD-6FP₂ has no active site available for other substrates.

ACKNOWLEDGEMENTS

The financial support from the National Science Council, Taiwan, R. O. C. is also gracefully acknowledged.

ABBREVIATIONS

XOD	=	xanthine oxidase
6FP	=	6-formylpterin
6CP	=	6-carboxylpterin
AFR	=	activity-flavin ratio
ES	=	enzyme-substrate complex

REFERENCES

- [1] Gallagher, E.P.; Kunze, K.L.; Stapleton, P.L.; Eaton, D.L. The kinetics of aflatoxin B1 oxidation by human cDNA-expressed and human liver microsomal cytochromes P450 1A2 and 3A4. *Toxicol. Appl. Pharma.*, **1996**, *141*, 595-606.
- [2] Luchter-Wasylewska, E. Cooperative kinetics of human prostatic acid phosphatase. *Biochim. et Biophys. Acta-Protein Struc. Mol. Enzym.* **2001**, *1548*, 257-264.
- [3] Njalsson, R.; Norgren, S.; Larsson, A.; Huang, C.S.; Anderson, M. E.; Luo, J. L. Cooperative binding of gamma-glutamyl substrate to human glutathione synthetase. *Biochem. Biophys. Res. Comm.* **2001**, *289*, 80-84.
- [4] Davidson, V.L.; Sun, D.P. Evidence for substrate activation of electron transfer from methylamine dehydrogenase to amicyanin. *J. Am. Chem. Soc.* **2003**, *125*, 3224-3225.
- [5] Johnson, J.L.; Cusack, B.; Davies, M.P.; Fauq, A.; Rosenberry, T.L. Unmasking tandem site interaction in human acetylcholinesterase. substrate activation with a cationic acetanilide substrate. *Biochemistry* **2003**, *42*, 5438-5452.
- [6] Koshland, Jr. D.E.; Stallcup W.B. Half of the sites reactivity and negative cooperativity- case of yeast glyceraldehyde-3-phosphate dehydrogenase. *J. Molecular Biol.* **1973**, *80*, 41-44.
- [7] Levitzki, A.; Stallcup, W.B.; Koshland, Jr. D.E. Half-of-sites reactivity and conformational states of cytidine triphosphate synthetase. *Biochemistry* **1971**, *10*, 3371-3378.
- [8] Hlavica, P.; Lewis, D.F.V. Allosteric phenomena in cytochrome P450-catalyzed monooxygenations. *Eur. J. Biochem.* **2001**, *268*, 4817-4832.
- [9] Karaoglu, D.; Kelleher, D.J.; Gilmore, R. Allosteric regulation provides molecular mechanism for preferential utilization of the fully assembled dolichol-linked oligosaccharide by the yeast oligosaccharyltransferase. *Biochemistry* **2001**, *40*, 12193-12206.
- [10] Enroth, C.; Eger, B.T.; Okamoto, K.; Nishino, T.; Nishino, T.; Pai, E.F. Crystal structures of bovine milk xanthine dehydrogenase and xanthine oxidase: Structure-based mechanism of conversion. *Proc. Natl. Acad. Sci. U. S. A.* **2000**, *97*, 10723-10728.
- [11] Hille, R. The mononuclear molybdenum enzymes. *Chem. Rev.*, **1996**, *96*, 2757-2816, and references cited therein.
- [12] Elion, G.B. The Purine Path to Chemotherapy. *Science*, **1989**, *244*, 41-47.
- [13] Lynch, M.J.; Grum, C.M.; Gallagher, K.P.; Bollin, S.F.; Deeb, M.; Morganroth, M.L. Xanthine oxidase inhibition attenuates ischemic-reperfusion lung injury. *J. Surg. Res.* **1988**, *44*, 538-544.
- [14] Millar, T.M.; Stevens, C.R.; Benjamin, N.; Eisenthal, R.; Harrison, R.; Blake, D.R. Xanthine oxidoreductase catalyses the reduction of nitrates and nitrite to nitric oxide under hypoxic conditions. *FEBS Lett.*, **1998**, *427*, 225-228.
- [15] Hille, R.; Anderson, R.F. Electron-transfer in milk xanthine oxidase as studied by pulse radiolysis. *J. Biol. Chem.* **1991**, *266*, 5608-5615.
- [16] Hille, R.; Massey, V. The equilibration of reducing equivalents within milk xanthine oxidase. *J. Biol. Chem.* **1986**, *261*, 1241-1247.
- [17] Hofstee, B.H.J. On the mechanism of inhibition of xanthine oxidase by the substrate xanthine. *J. Biol. Chem.* **1955**, *216*, 235-244.
- [18] Rubbo, H.; Radi, R.; Prodanov, E. Substrate inhibition of xanthine oxidase and its influence on superoxide radical production. *Biochim. Biophys. Acta.* **1991**, *1074*, 386-391.
- [19] Tai, L.A.; Hwang, K.C. Cooperative catalysis in the homodimer subunits of xanthine oxidase. *Biochemistry* **2004**, *43*, 4869-4876.
- [20] Segel, I.H. *Enzyme Kinetics: Behavior and Analysis of Rapid Equilibrium and Steady-State Enzyme Systems*. John Wiley & Sons, Inc.: New York, **1993**, Chap. 7.
- [21] Kim, J.H.; Ryan, M.G.; Knaut, H.; Hille, R. The reductive half-reaction of xanthine oxidase - the involvement of prototropic equilibria in the course of the catalytic sequence. *J. Biol. Chem.* **1996**, *271*, 6771-6780.
- [22] Hussein, A.S.; Chacón, M.R.; Smith, A.M.; usado-Acevedo, R.; Selkirk, M.E. Cloning, expression, and properties of a nonneuronal secreted acetylcholinesterase from the parasitic nematode *nippostrongylus brasiliensis*. *J. Biol. Chem.* **1999**, *274*, 9312-9319.
- [23] Masson, P.; Schopfer, L.M.; Bartels, C.F.; Froment, M.T.; Ribes, F.; Nachon, F.; Lockridge, O. Substrate activation in acetylcholinesterase induced by low pH or mutation in the cation subsite. *Biochimica et Biophysica Acta*, **2002**, *1594*, 313-324.
- [24] Dixon, H.B.F.; Tipton, K.F. Negative cooperative ligand binding. *Biochem. J.* **1973**, *133*, 837-842.
- [25] Wharton, C.W.; Cornish-Bowden, A.; Brocklehurst, K.; Crook, E.M. Comparison of experimental binding data and theoretical models in proteins containing subunits. *Biochem. J.* **1974**, *141*, 365-381.
- [26] Okamoto, K.; Matsumoto, K.; Hille, R.; Eger, B.T.; Pai, E.F.; Nishino, T. The crystal structure of xanthine oxidoreductase during catalysis: Implications for reaction mechanism and enzyme inhibition. *Proc. Natl. Acad. Sci. U.S.A.*, **2004**, *101*, 7931-7936.
- [27] Pauff, J.M.; Zhang, J.; Bell, C.E.; Hille, R. Substrate orientation in xanthine oxidase - crystal structure of enzyme in reaction with 2-hydroxy-6-methylpurine. *J. Biol. Chem.* **2008**, *283*, 4818-4824.
- [28] Massey, V.; Komai, H.; Palmes, G. On mechanism of inactivation of xanthine oxidase by allopurinol and other pyrazolo 3,4-dipyrimidines. *J. Biol. Chem.* **1970**, *245*, 2837-2844.
- [29] The kinetic model and velocity equation for heterosubstrate cooperative interactions will be derived and discussed in later publications.
- [30] Avis, P.G.; Bergal, P.; Bray, B.C. Cellular Constituents- The Chemistry of Xanthine Oxidase 1. The Preparation of a Crystalline Xanthine Oxidase from Cows Milk. *J. Chem. Soc.* **1955**, 1100-1104.